NOTES AND CORRESPONDENCE

Bottom-Trapped Rossby Waves in an Exponentially Stratified Ocean

Robert O. Reid and Ou Wang*

Department of Oceanography, Texas A&M University, College Station, Texas

4 June 2003 and 5 September 2003

ABSTRACT

The well-known Rhines theory of bottom-trapped topographic Rossby waves (TRW) in a uniformly stratified ocean over a sloping seabed, and its dispersion relation between wave frequency and wavenumber components, have served a very useful purpose in prompting recognition of the existence of TRW in the ocean and in motivating the search for sources of such disturbances. However, in quantitative studies of backward ray tracing of bottom-trapped Rossby waves for source search purposes, a realistic profile of the buoyancy frequency $N(z)$ within the water column ought to be taken into account. Toward this goal an analytic solution for linear, quasigeostrophic, topographic Rossby waves for an ocean having regionally distinct exponential profiles of buoyancy frequency is offered.

1. Introduction

Observational evidence of bottom-trapped topographic Rossby waves (TRW) in the stratified ocean has received increasing attention since the appearance of the theoretical monograph by Rhines (1970). Of particular interest in such studies has been locating sources for the excitation and radiation of TRW observed in the deep continental rise area northwest of the Gulf Stream in the North Atlantic and west of the Loop Current in the Gulf of Mexico (Johns and Watts 1986; Hamilton 1984, 1990; Pickart and Watts 1990; Hogg 1988; Nowlin et al. 2001). To quantify the location of energy sources from observed sites of TRW, backward ray tracing methodology has been invoked (Pickart 1995; Oey and Lee 2002). These studies make use of the analytic TRW dispersion relation for a uniformly stratified ocean put forth by Rhines (1970), but carefully interpreted in these recent studies for general topography. However, the serious shortcoming of the currently used analytic TRW dispersion relation is the restriction to *vertically uniform* buoyancy frequency (N) over the water column. Even in the subthermocline regions of the ocean, $N(z)$ is more nearly exponential than uniform (Fig. 1). Rhines (1970) recognized this and even addressed possible modification for the effect of variable N. Because of its simplistic elegance and convenience, however, the Rhines (1970) dispersion relation for uniform N has persisted as an approximation for the ocean.

The purpose of this note is to offer an alternative TRW dispersion relation that applies to an ocean having an exponential $N(z)$ profile. Even for the exponential case one can get an analytic solution, and this should facilitate its use in ray tracing studies. We demonstrate that the exponential approximation for $N(z)$ leads to dispersion relations for TRW that closely match those based on typical observed $N(z)$ for the Gulf of Mexico and the Sargasso Sea. For the observed stability profiles we make use of a numerical algorithm as in the monograph of Charney and Flierl (1981). The comparisons confirm that: (i) the fitted exponential profiles of N give dispersion results close to those derived from historic hydrographic data and (ii) the realistic $N(z)$ give TRW dispersion results significantly different from that of uniform N. We use the exponential $N(z)$ to derive curves of the maximum dimensionless wave frequency (for given wavelength) versus dimensionless wavelength for different values of the parameter μ, whose reciprocal quantifies the relative e-folding scale of N. The Rhines solution is a special case for $\mu = 0$. Finally a typical example is given of contours of wave frequency in wavenumber space based on the exponential N profile for comparison with a similar plot based on uniform N. The differences are significant in terms of the contour patterns and the implied field of group velocity that is required in wave tracing studies.

* Current affiliation: Jet Propulsion Laboratory, California Institute of Technology, Pasadena, California.

Corresponding author address: Prof. Robert O. Reid, Department of Oceanography, Texas A&M University, College Station, TX 77843-3146.
E-mail: rreid@ocean.tamu.edu

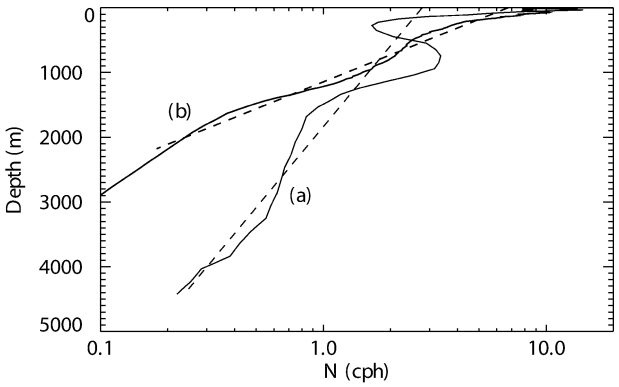

FIG. 1. Examples of domain-averaged buoyancy frequency (N) profiles (full curves) for (a) the Sargasso Sea from Arango and Reid (1990), and (b) the Gulf of Mexico from Current (1993). See text (section 2c) for fitted exponential profiles (dashed) for selected water depths at 4000 and 2000 m in the Sargasso Sea and the Gulf of Mexico, respectively.

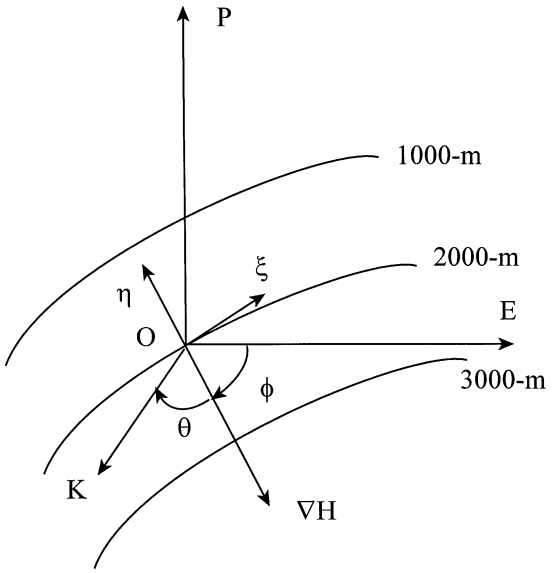

FIG. 2. Schematic diagram (for Northern Hemisphere) showing water depth contours, the local depth gradient vector (∇H), the local wavenumber (phase propagation) vector ($\mathbf{K}$), the subtended angle (θ), and the local along-slope (ξ) and cross-slope (η) coordinates, where ξ is positive in the anticyclonic sense (for given hemisphere) and η is positive in the upslope sense. The eastward and poleward coordinate vectors are respectively O–E and O–P, and ϕ is the angle between vector (O–E) and ∇H. Both ϕ and θ are positive in the anticyclonic sense (for a given hemisphere).

2. Topographic Rossby wave dynamics

a. The TRW eigenvalue problem

The governing equation for planetary and/or topographic Rossby waves in a stratified ocean with buoyancy frequency $N(z)$ is the linear quasigeostrophic vorticity equation (Rhines 1970; Charney and Flierl 1981; Pickart 1995):

$$\{p_{xx} + p_{yy} + [p_z(f_o/N)^2]_z\}_t + \beta p_x = 0, \qquad (1)$$

where x, y, and z are respectively position coordinates positive eastward, northward, and upward (relative to the mean sea surface); t is time; p is pressure anomaly; and $f = f_o + \beta y$ is the Coriolis parameter. The boundary conditions are taken as a rigid lid at the sea surface and flow tangential to the sloping seabed:

$$p_{zt} = 0 \qquad \text{at } z = 0 \quad \text{and} \qquad (2)$$

$$p_{zt} = (N^2/f_o)J(p, H) \quad \text{at } z = -H, \qquad (3)$$

where H is the local depth. If the seabed slope is considered plane (uniform slope), then simple wave solutions have the separable form:

$$p = F(z)\exp[i(kx + ly - \omega t)], \qquad (4)$$

in which k and l are respectively the x and y components of the vector wavenumber and ω is frequency.

The vertical structure function for p should satisfy the eigenvalue problem:

$$[(f_o/N)^2F_z]_z = \lambda^2 F, \qquad (5)$$

$$F_z = 0 \qquad \text{at } z = 0, \qquad (6)$$

and

$$\omega F_z = -(N^2/f_o)(kH_y - lH_x)F \quad \text{at } z = -H, \qquad (7a)$$

where λ^2 is the separation constant (positive for the bottom-trapped TRW mode). The term $(kH_y - lH_x)$ in (7) is the z component of $\mathbf{K} \times \nabla H$, where $\mathbf{K}$ is the horizontal wavenumber vector (Fig. 2). Following Oey and Lee (2002), this can also be expressed as $(\alpha K \sin\theta)$, where α is the seabed slope magnitude $|\nabla H|$, K is the wavenumber magnitude, and θ is the clockwise angle that vector $\mathbf{K}$ makes with ∇H, for the Northern Hemisphere (Fig. 2). Thus (7a) can be expressed in the more useful form

$$\omega F_z = -(N^2/f_o)\alpha K \sin\theta F \quad \text{at } z = -H. \qquad (7b)$$

Last, relation (1) with (4) and (5) gives the following closure relation among the various wave parameters:

$$k^2 + l^2 + \beta k/\omega = \lambda^2. \qquad (8)$$

Like (7b), this can be written in a more useful form involving the polar components (K, θ) of the wavenumber vector:

$$K^2 = \lambda^2 - (\beta K/\omega)\cos(\theta + \phi), \qquad (9)$$

where ϕ is the orientation angle of ∇H (see Fig. 2).

It should be emphasized that the separable solution outlined above assumes that the seabed is a sloping plane. In a practical sense, this implies that the application of the resulting dispersion relation for the bottom-trapped waves ought to be restricted to wavelengths that are small compared with typical scales of the bottom topography. This is why smoothing of bottom topography in TRW ray tracing studies is common (Pickart

1995; Oey and Lee 2002). We also note that it is only those TRW having small wavelengths (less than 200 km) that are strongly bottom trapped.

b. Analytic solution for exponential N(z)

We consider here possible analytic solutions of the eigenvalue problem (5)–(8) for a water column of depth H having the following exponential profile:

$$N(z) = N_b \exp[(z + H)/h], \tag{10}$$

where h is an e-folding scale and N_b denotes the value of N at the seabed. It will be helpful to transform (5) using

$$\zeta = (\lambda h N_b/f_o) \exp[(z + H)/h] \tag{11}$$

as the independent coordinate and

$$W = (f_o/N)^2 dF/dz \tag{12a}$$

as the dependent variable. Using (5), this implies that

$$dW/dz = \lambda^2 F. \tag{12b}$$

Then (5) takes the form of a Bessel equation of zero order:

$$d^2W/d\zeta^2 + \zeta^{-1} dW/d\zeta - W = 0, \tag{13a}$$

with boundary conditions

$$W = 0 \quad \text{at } \zeta = \zeta_o \quad \text{and} \tag{13b}$$

$$W = -\alpha K N_b/(\omega\lambda) dW/d\zeta \sin\theta \quad \text{at } \zeta = \zeta_b, \tag{13c}$$

where ζ_o and ζ_b are respectively the values of ζ at the sea surface and the seabed.

A solution of (13a) that satisfies (13b) is

$$W = \mathrm{I}_0(\zeta_o)\mathrm{K}_0(\zeta) - \mathrm{K}_0(\zeta_o)\mathrm{I}_0(\zeta), \tag{14}$$

where $\mathrm{K}_n(\zeta)$ and $\mathrm{I}_n(\zeta)$ are the modified (evanescent) Bessel functions of order n. Using the properties $\mathrm{I}_0'(\zeta) = \mathrm{I}_1(\zeta)$ and $\mathrm{K}_0'(\zeta) = -\mathrm{K}_1(\zeta)$, the bottom boundary condition then gives the following relation for the wave frequency:

$$\omega/\alpha N_b = [(K/\lambda) \sin\theta]/\Gamma, \tag{15}$$

where

$$\Gamma = [\mathrm{I}_0(\zeta_o)\mathrm{K}_0(\zeta_b) - \mathrm{K}_0(\zeta_o)\mathrm{I}_0(\zeta_b)] \times [\mathrm{I}_0(\zeta_o)\mathrm{K}_1(\zeta_b) + \mathrm{K}_0(\zeta_o)\mathrm{I}_1(\zeta_b)]^{-1}. \tag{16}$$

The parameters ζ_b and ζ_o can be expressed in the form

$$\zeta_b = \lambda^* \mu^{-1} \quad \text{and} \quad \zeta_o = \lambda^* \mu^{-1} \exp(\mu), \tag{17a,b}$$

where

$$\mu = H/h \quad \text{and} \quad \lambda^* = \lambda H N_b/f_o. \tag{18a,b}$$

Thus Γ is a function of a scaled λ and the aspect ratio μ whose reciprocal is the relative e-folding scale for the exponential N profile.

Relation (9) with (15) yields the following parametric form of the dispersion relation for TRW in an ocean with exponential $N(z)$:

$$KHN_b/f_o = \lambda^* B \quad \text{and} \tag{19a}$$

$$\omega/\alpha N_b = (B \sin\theta)/\Gamma(\lambda^*, \mu), \tag{19b}$$

where

$$B = \{1 + R[\Gamma(\lambda^*, \mu)/\lambda^*](\sin\phi - \cos\phi \cot\theta)\}^{1/2}, \tag{19c}$$

and $R = \beta H/\alpha f_o$, which is the ratio of planetary to topographic beta. For the case in which topographic beta ($\alpha f_o/H$) greatly exceeds β, then B is nearly unity, the scaled λ can be replaced by the similarly scaled K, and the dispersion relation simplifies to the following approximation

$$\omega/\alpha N_b = (\sin\theta)/\Gamma(KHN_b/f_o, \mu). \tag{20}$$

From the asymptotic properties of the modified Bessel functions for large arguments, it can be shown that $\Gamma(\lambda^*, \mu)$ reduces to $\tanh\lambda^*$ as μ approaches zero. Thus the commonly used Rhines (1970) dispersion relation based on uniform $N(\mu = 0)$ is a *special case* of the more general solution (19a)–(19c) that pertains to the exponential N profile. On the other hand, if μ is held fixed but $(KHN_b/f_o)^{-1}$ approaches zero and β is neglected, then the following approximation applies:

$$\omega/\alpha N_b = [1 + 0.5\mu(KHN_b/f_o)^{-1}] \sin\theta \tag{21}$$

for bottom-trapped TRW of very short wavelength. At the other extreme of very long TRW (KHN_b/f_o approaching zero) with β neglected then

$$\omega = \alpha f_o/KH, \tag{22}$$

which is independent of N and hence of μ. The latter approximation applies only to purely barotropic (uniform F) topographic Rossby waves and therefore is only of academic interest here.

The maximum wave frequency (ω_m) for fixed K occurs for $\sin\theta = 1$. For $\beta = 0$ we show the quantity $\omega_m/\alpha N_b$ versus the scaled wavelength $(KHN_b/f_o)^{-1}$ in Fig. 3 for selected μ based on (20). The lowest curve ($\mu = 0$) corresponds to the Rhines dispersion relation for uniform N. The initial slope at zero wavelength is zero, while other curves have the initial slope $\mu/2$ in accord with (21). This is an important generalization since it allows for a positive ξ component of group velocity for short wavelength TRW (discussed further in section 3b).

c. Numerical solution for general N(z)

For observed $N(z)$ profiles as in Fig. 1, the eigenvalue problem (5)–(8) requires numerical solution as in Charney and Flierl (1981). Our numerical code is similar to that of Arango and Reid (1990) and Current (1993) with adaptation to the boundary condition (7) and the constraint (8). This code computes F and W at each discrete level so as to facilitate use of the boundary conditions.

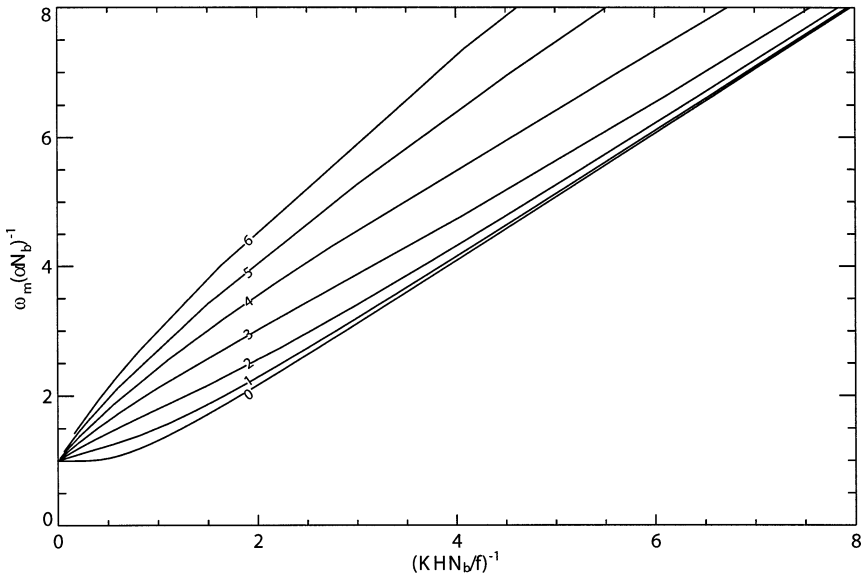

FIG. 3. The maximum scaled frequency ($\omega_m/\alpha N_b$), for given K, vs the scaled wavelength (KHN_b/f)$^{-1}$ for selected values of parameter $\mu(=H/h)$ characterizing exponential profiles of N having bottom value of N_b, as determined by the analytic solution (20) for the case of zero planetary beta. Note that the Rhines solution for uniform N corresponds to the special case of $\mu = 0$.

For the case of nonzero R, the code requires an iterative convergence for λ and ω for given K, while for $R = 0$ no iteration is required since $\lambda = K$ and evaluation of ω involves direct use of the seabed boundary condition (7b). The numerical code used here was developed to compute bottom-trapped and surface-trapped dynamic modes over a sloping seabed as in Charney and Flierl (1981) to allow decomposition of measured currents at a mooring site near 27°N, 90°W in the Gulf of Mexico (Nowlin et al. 2001). (A paper elaborating on that study is in preparation.)

As a test of the numerical model, we applied it to the exponential profile shown by the dashed line for the Gulf of Mexico case in Fig. 1b. This profile is an approximation for a mooring site in the Gulf of Mexico at about 27°N, in 2000-m water depth, bottom slope of 0.016 downward toward the south, seabed N of 0.24 cph, and an e-folding scale of 600 m (hence μ is about 3.3). The resulting scaled ω_m versus the scaled wavelength from the numerical code is shown by the circles in Fig. 4 for three selected values of R (0, 0.1, and 0.2). The full lines are determined by the analytic solution (19a,b,c) for $\mu = 3.3$. These results, and a similar test for the case of $\mu = 0$ (not shown) represent partial confirmation of the numerical model. Figure 4 also serves as a supplement to Fig. 3, to illustrate the effect of planetary beta on the maximum TRW wave frequency versus wavelength. For small wavelengths the planetary beta has small effect.

We now consider two examples of real oceanic stability profiles for which the TRW dispersion relations can be represented quite well by those derived from the fitted exponential $N(z)$. We find that fitted profiles of form (10) that have the same N_b as the actual profile (as in Fig. 1) tend to yield the best rendition of the TRW dispersion relation. Our numerical code based on (5)–(8) was employed to determine the maximum wave frequency ω_m (i.e., taking sin $\theta = 1$) as a function of K for the actual N profiles in Fig. 1. We then carried out similar calculations for the fitted exponential profiles shown in Fig. 1. The results are shown in Fig. 5, whose caption gives the latitude, N_b, h, and bottom slope α for the two cases. The exponential approximations of N for the Sargasso Sea and Gulf of Mexico examples have, respectively, μ values of about 2.2 and 3.3, and the associated dispersion relations are quite distinct (Fig. 5). However, the dispersion relations based on the actual N profile and its exponential fit for a given oceanic basin are very close. In contrast, the dispersion relation based on uniform N, shown as the dashed curve in Fig. 5, is quite different from its counterpart for the Gulf of Mexico case.

Figure 5 includes insets showing the vertical structure for the two oceanic examples. As is well known, the bottom trapping associated with TRW modes is most pronounced for short wavelengths. The parameter λ^{-1} (or K^{-1} for the case of negligible R) when divided by the column average value of N/f_o is a measure of the vertical trapping scale for the TRW.

3. K-space dispersion and group velocity

a. Example dispersion diagrams in 2D wavenumber space

The TRW wave frequency ω for the propagation vector **K** specified in terms of magnitude K and angle θ

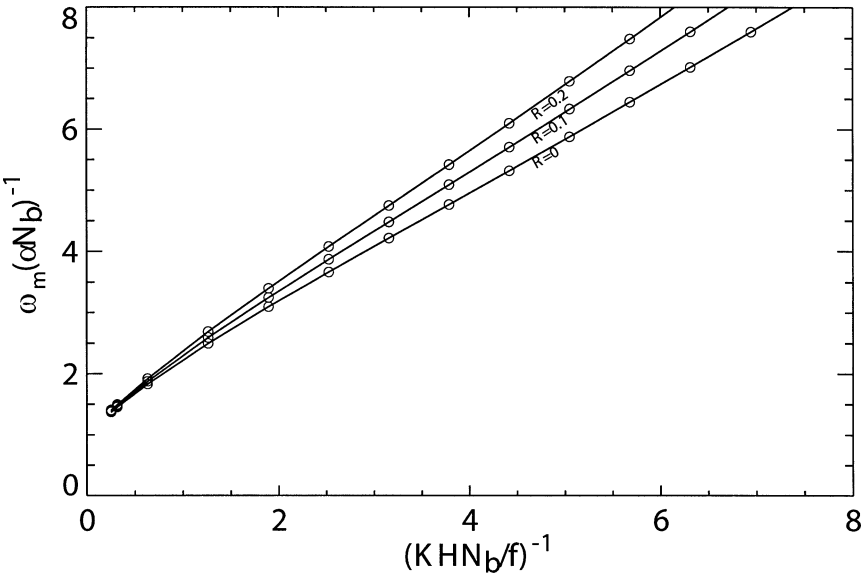

FIG. 4. Maximum scaled frequency ($\omega_m/\alpha N_b$) of TRW, for given K, vs the scaled wavelength $(KHN_b/f)^{-1}$ for a water column with $\mu = 3.3$ and an exponential buoyancy frequency (N). Full curves are based on the analytic relations (19a)–(19c). The circles are based on our numerical code. Parameter R is the ratio of planetary to topographic beta.

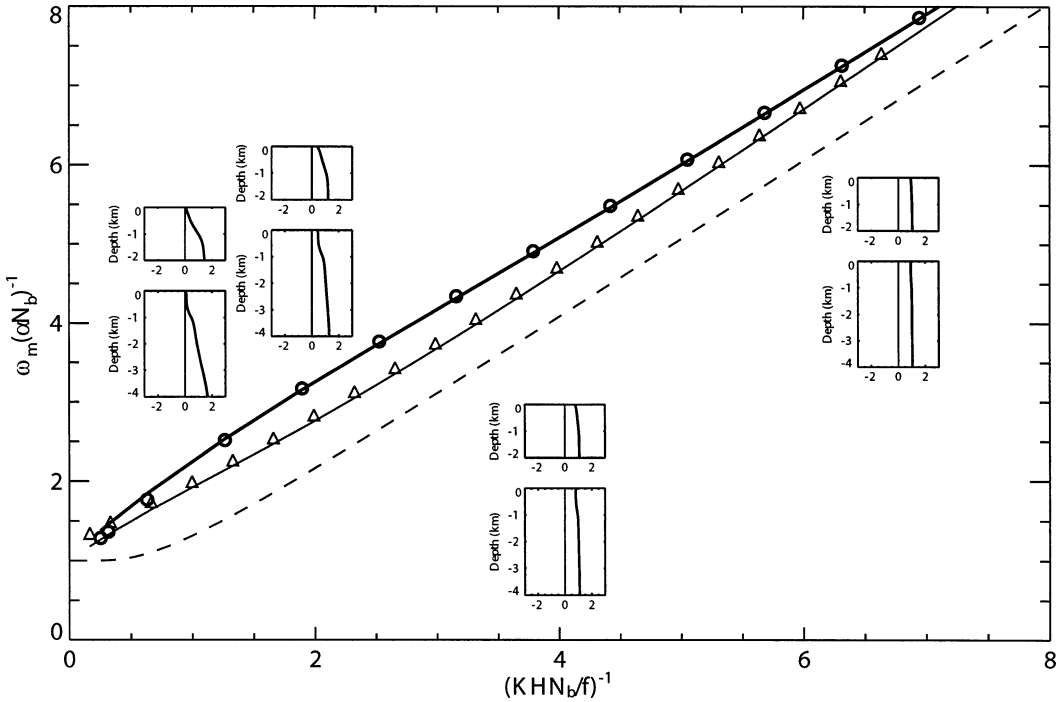

FIG. 5. Comparison of maximum scaled frequency ($\omega_m/\alpha N_b$), for given K, vs the scaled wavelength $(KHN_b/f)^{-1}$ for actual $N(z)$ (symbols) and exponential fit (full curves), having common bottom buoyancy frequency: (a) Sargasso Sea (triangles) at about 37°N with $H = 4000$ m, $N_b = 0.3$ cph, $h = 1800$ m, $\alpha = 0.011$; and (b) Gulf of Mexico (circles) at about 27.25°N with $H = 2000$ m, $N_b = 0.24$cph, $h = 600$ m, $\alpha = 0.016$. Full curves are determined by our analytic solution (19a)–(19c) for TRW including the effect of planetary beta. Symbols are based on the use of our numerical code with actual $N(z)$. The relation for uniform N (equal to the bottom value), for case (b) but with $R = 0$, is also shown (dashed) for comparison. Insets show sample vertical structure of the TRW mode for selected scaled wavelengths and the two different depths.

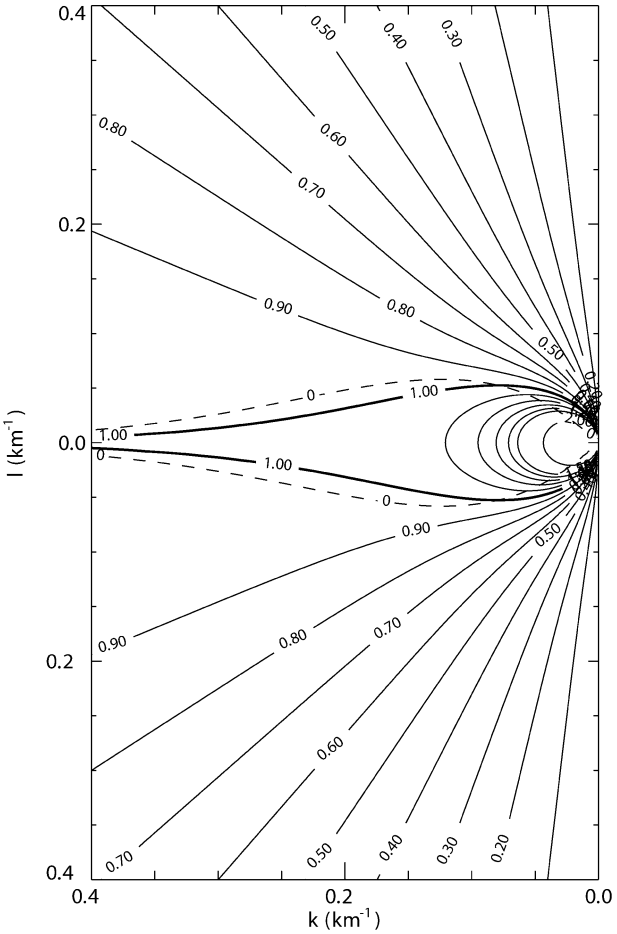

FIG. 6. Example dispersion diagram for TRW having $\mu = 0$ (uniform profile of N) showing contours of scaled frequency ($\omega/\alpha N_b$) in wavenumber space k vs l for the case of zero planetary beta and a seabed sloping downward toward the equator. The latitude is 27.25°N, $N = 0.24$ cph, $\alpha = 0.016$, and $H = 2000$ m. The dashed curve corresponds to zero east–west group velocity (or more generally zero group velocity component in the along-slope sense).

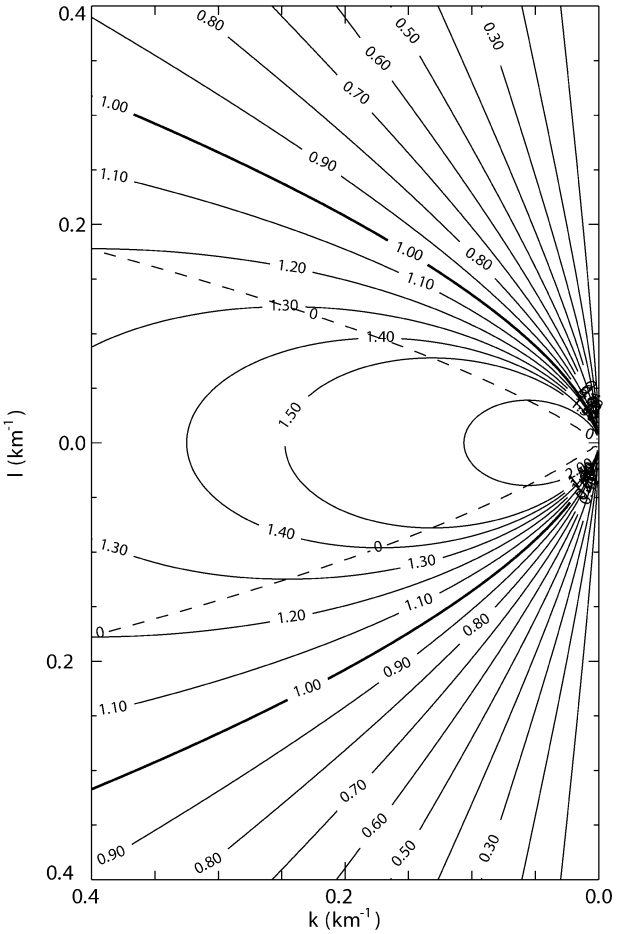

FIG. 7. Example dispersion diagram for TRW having $\mu = 3.3$ (exponential profile as in Fig. 1b) showing contours of scaled frequency ($\omega/\alpha N_b$) in wavenumber space k vs l for the case of zero planetary beta and a seabed sloping downward toward the equator. The latitude is 27.25°N, $N_b = 0.24$ cph, $\alpha = 0.016$, and $H = 2000$ m. The dashed curve corresponds to zero east–west group velocity (or more generally zero group velocity component in the along-slope sense).

(Fig. 2) is given by $\omega = \omega_m(K)\sin\theta$, where $\omega_m(K)$ can be computed for $R = 0$ from the analytic relation (20) for given μ, or from (20) for the case of $\mu = 0$ taking $\Gamma = \tanh(\lambda^*)$. The components of **K** in natural ξ, η coordinates (Fig. 2) are respectively $-K\sin\theta$ and $-K\cos\theta$. For simplicity in the following illustrations, we will consider the case in which H is increasing toward the equator; then the ξ and η components are the same as the k and l components, respectively.

Figures 6 and 7 give example plots for contours of ω in wavenumber space for two examples. Figure 6 is for uniform N profiles ($\mu = 0$) on an f plane ($\beta = 0$), while Fig. 7 is for the case where $\mu = 3.3$ on an f plane. Other parameters for both cases are for conditions as stipulated in the captions. The plots show contours of scaled frequency, but the wavenumber components are dimensional with maximum magnitude of k and l corresponding to a minimum wave length of order 15 km. The value of the maximum scaled frequency at infinite wavenumber is unity (or αN_b in dimensional form).

b. Group velocity

The group velocity is defined by the gradient of ω in wavenumber space and hence is normal to the frequency contours and is directed toward larger values of the scaled frequency. The dashed line in Figs. 6 and 7 is the zero value of east–west group velocity. Hence those TRW that have only a westward component of group velocity lie outside (above and below) the dashed lines in the dispersion diagrams. Such waves can be refracted by variable topography and even reflected by steep escarpments having an east–west orientation. However, only TRW that fall within the dashed lines can be reflected by north–south-oriented escarpments.

The relations for determination of ray tracing and changes in the properties of the bottom-trapped Rossby waves due to refraction are clearly summarized in Oey and Lee (2002). The group velocity **G** and its dependence on the environmental parameters play a central role in determining the ray paths and the changes in wave properties. As an alternative to graphical evaluation of $\nabla_k\omega$, relations (19a)–(19c) or (20) for the $\beta = 0$ approximation, allow one to determine the polar components (K, θ) from

$$G_K = \partial\omega/\partial K \quad \text{and} \quad G_\theta = K^{-1}\partial\omega/\partial\theta, \qquad (23)$$

which can be converted readily to Cartesian components. While the wave frequency is an invariant along a ray path, the wavenumber vector and consequently the group velocity vector will be subject to changes associated with the environmental parameters that govern the dispersion relation. These parameters include primarily H, ∇H, N_b, and μ. In the existing ray tracing studies based on the Rhines dispersion relation ($\mu = 0$), the value of N is taken as an average over a selected subthermocline depth range. Possibly for this reason, Oey and Lee (2002) express some concern about the uncertainty of the buoyancy frequency employed in their study.

4. Closing remarks

We offer a generalized analytic dispersion relation for bottom-trapped Rossby waves that is based on the representation of the buoyancy frequency profile $N(z)$ by an exponential relation. We have shown that the exponential representation of $N(z)$ gives a surprisingly good approximation of the dispersion relation corresponding to typical real profiles of N for the Gulf of Mexico and the Sargasso Sea. Illustrations are given for two special cases. Figure 7 is for a typical water column in the Gulf of Mexico. Figure 6 is for a water column that probably does not exist in the upper 6000 m of the ocean. There is a striking contrast in these example 2D dispersion diagrams, especially in terms of the implied behavior of the group velocity.

For the suggested new dispersion relation, based on an exponential profile of N, there is no ambiguity as to the scaling for the wave frequency—it is the bottom value of N. This can make a significant difference in the maximum frequency of the short-wavelength, strongly bottom-trapped, topographic Rossby waves from that presently estimated. On the other hand, the additional parameter μ, which characterizes the degree of variation of N over the water column, gives a definitive extra degree of freedom in determining the resulting dispersion relation. Note for example that cases (a) and (b) of Fig. 1 have comparable values of N_b but have quite different values of μ as well as H. Thus the dispersion relations, even in scaled form, differ mainly because of the difference in the μ value.

Acknowledgments. The first author acknowledges the inspiration of prior studies with Dr. Hernan G. Arango and Dr. Carole L. Current on dynamic modes in the Gulf of Mexico and the North Atlantic. Both authors thank prior support by the Minerals Management Service of the U.S. Department of Interior in the Deepwater Synthesis study that motivated the present paper. Last, the second author was supported in his postdoctoral studies by Office of Naval Research through a subcontract of a grant between Texas A&M University and Mississippi State University, and by Navy National Ocean Partnership Program through a subcontract of a grant between Texas A&M University and University of Rhode Island.

REFERENCES

Arango, H. G., and R. O. Reid, 1990: A generalized reduced-gravity ocean model: An application for the short-term evolution and prediction of surface mesoscale fields. Technical report prepared for the United States Coast Guard, Project 5800-17, Department of Oceanography, Texas A&M University, 154 pp.

Charney, J. G., and G. R. Flierl, 1981: Oceanic analogues of large-scale atmospheric motions. *Evolution of Physical Oceanography*, B. A. Warren and C. Wunsch, Eds., The MIT Press, 504–548.

Current, C. L., 1993: Empirical vertical structure of density anomaly in the Gulf of Mexico. M.S. thesis, Dept. of Oceanography, Texas A&M University, 143 pp.

Hamilton, P., 1984: Topographic and inertial waves on the continental rise of the Mid-Atlantic Bight. *J. Geophys. Res.,* **89** (C1), 695–710.

——, 1990: Deep currents in the Gulf of Mexico. *J. Phys. Oceanogr.,* **20,** 1087–1104.

Hogg, N. G., 1988: Stochastic wave radiation by the Gulf Stream. *J. Phys. Oceanogr.,* **18,** 1687–1701.

Johns, W. L., and D. R. Watts, 1986: Time scales and structure of topographic Rossby waves and meanders in the deep Gulf Stream. *J. Mar. Res.,* **44,** 267–290.

Nowlin, W. D., Jr., A. E. Jochens, S. F. DiMarco, R. O. Reid, and M. K. Howard, 2001: Deepwater physical oceanography reanalysis and synthesis of historical data: Synthesis report. OCS Study MMS 2001-064, U.S. Department of the Interior, Minerals Management Service, Gulf of Mexico OCS Region, New Orleans, LA, 528 pp.

Oey, L.-Y., and H.-C. Lee, 2002: Deep eddy energy and topographic Rossby waves in the Gulf of Mexico. *J. Phys. Oceanogr.,* **32,** 3499–3527.

Pickart, R. S., 1995: Gulf Stream–generated topographic Rossby waves. *J. Phys. Oceanogr.,* **25,** 574–586.

——, and D. R. Watts, 1990: Deep western boundary current and variability at Cape Hatteras. *J. Mar. Res.,* **48,** 765–791.

Rhines, P., 1970: Edge-, bottom-, and Rossby waves in a rotating stratified fluid. *Geophys. Fluid Dyn.,* **1,** 273–302.